INTERNATIONAL JOURNAL FOR NUMERICAL METHODS IN FLUIDS, VOL. 11, 677–695 (1990)

SIMULATION OF TURBULENCE WITH TRANSIENT MEAN

C. BÈGUE

AMD-BA, Division Études Avances, 78 quai Marcel Dassauft, St Cloud, France

B. CARDOT AND C. PARÈS

INRIA, F-78153 Le Chesnay, France

AND

O. PIRONNEAU

Université Paris 6 and INRIA, F-78153, Le Chesnay, France

SUMMARY

In general the k–ε turbulence model is used for stationary turbulent mean flow. First we review some of the hypotheses for the derivation of the model. Then we study it from the point of view of the numerical analyst (positivity of k and ε, boundedness, etc.). Finally we analyse an extension called MPP, specially derived for transient mean flow. The rest of the paper is devoted to a robust (stable) numerical implementation of these models and several tests for the flow behind a cylinder.

KEY WORDS Turbulence Incompressible Navier–Stokes Finite element k–epsilon Transient flow

1. INTRODUCTION

The Navier–Stokes equations describe accurately the motion of Newtonian incompressible fluids:

$$u_{,t}+u\nabla u+\nabla p-\nu\Delta u=f, \qquad \nabla\cdot u=0. \tag{1}$$

With appropriate boundary conditions, (1) defines the velocity field u and the pressure field p uniquely;[1,2] f is the density of external volumic forces acting on the flow.

To solve the Navier–Stokes equations numerically with the finite element method, (1) must be written in variational form. For instance, with Dirichlet boundary conditions the initial boundary value problem in variational form is

$$(u_{,t}, v)+(u\nabla u, v)+\nu(\nabla u, \nabla v)=(f, v), \quad \forall v\in J_0(\Omega), \tag{2}$$

$$u(0)=u^0, \qquad u-u_\Gamma\in J_0(\Omega), \tag{3}$$

where

$$J(\Omega)=\{u\in H^1(\Omega)^n:\nabla\cdot u=0\},\ J_0(\Omega)=\{u\in J(\Omega):u|_\Gamma=0\}. \tag{4}$$

Ω denotes the computational domain, Γ its boundary, (a, b) is the integral of $a(x)\cdot b(x)$ on Ω and $H^1(\Omega)^n$ is the Sobolev space of vector-valued functions on $\mathbb{R}^n$ with square-integrable derivatives.

0271–2091/90/130677–19$09.50

Received April 1989
Revised March 1990

To discretize (2), (3) one simply replaces (4) by a finite-dimensional space J_h: find $u_h \in J_h$ such that

$$(u_{h,t}, v_h) + (u_h \nabla u_h, v_h) + \nu(\nabla u_h, \nabla v_h) = (f, v_h), \quad \forall v_h \in J_{0h}, \tag{5}$$

$$u_h(0) = u_h^0, \qquad u_h - u_{\Gamma_h} \in J_{0h}, \tag{6}$$

$$J_h = \{v_h \in V_h : (\nabla \cdot v_h, q_h) = 0 \quad \forall q_h \in Q_h\}. \tag{7}$$

We shall denote by J_{0h} the set of functions of J_h which are zero on the boundary Γ_h of the computational domain, and similarly

$$V_{0h} = \{v_h \in V_h : v_h|_{\Gamma_h} = 0\}. \tag{8}$$

Here h is a parameter such that $J_h \to J$ as h tends to zero; in the finite element context it is the size of the elements. One possible choice for V_h, Q_h is[3,4] the so-called mini-element,[5] where Q_h is the space of continuous piecewise linear functions on a triangulation (tetrahedrization in 3D) of Ω and where V_h is the space of continuous vector-valued functions also piecewise linear but on the triangulation deduced from T_h by dividing each element in three (four in 3D) from its centre of gravity.

Before time discretization, (5), (7) is a set of non-linear ODEs for which one can prove the following error estimates:[6]

$$\begin{aligned} \|u - u_h\|_{L^2(0,T;H_0^1(\Omega))} &\leqslant C\nu^{-1} h \|u \nabla u\|_0, \\ \|u - u_h\|_{L^2(]0,T[\times\Omega)} &\leqslant C\nu^{-1} h^2 \|u \nabla u\|_0. \end{aligned} \tag{9}$$

From the Prandtl equations one can estimate $\|u\nabla u\|_0$ in the boundary layers; similarly, if Kolmogorov's 5/3 law holds, one also reaches an estimate for $\|u\nabla u\|_0$. In both cases one finds that it is of order $\nu^{-1/4}$ when the equations are scaled so that u and Ω are of order unity (i.e. ν^{-1} is the Reynolds number).

Therefore (9) tells us that a reasonable precision will be achieved only if $h \ll \nu^{5/8}$. However, for practical applications the Reynolds number is usually larger than 10^6, so at least 1000 points in each spatial direction are required. Since one cannot afford such fine grids, turbulence modelling must be introduced.

2. TURBULENCE MODELLING

2.1. Reynolds' hypothesis

One approach to turbulence modelling is to consider the initial value problem for the Navier–Stokes equations with random initial data:

$$u_{,t} + u\nabla u + \nabla p - \nu \Delta u = 0, \qquad \nabla \cdot u = 0 \quad \text{in } \Omega \times]0, T[, \tag{10}$$

$$u(x, 0) = u^0(x) + w(x, \omega), \qquad u|_\Gamma = u_\Gamma, \tag{11}$$

where $w(x_0, .)$ is random with known statistics. Let $\langle\ \rangle$ denote the averaging operator (expected values). To compute $\langle u \rangle$ one replaces u by $u + u'$ in (10) (the mean of u is also denoted by u):

$$u_{,t} + u\nabla u + \nabla p - \nu \Delta u + \nabla \cdot u' \otimes u' = -(u'_{,t} + u'\nabla u + u\nabla u' + \nabla p' - \nu \Delta u'), \tag{12}$$

$$\nabla \cdot u' + \nabla \cdot u = 0, \tag{13}$$

because $u'\nabla u' = \nabla \cdot (u' \otimes u')$ when $\nabla \cdot u' = 0$. Now the averaging operator is applied to (12) and the Reynolds equations are found:

$$u_{,t} + u\nabla u + \nabla p - \nu \Delta u + \nabla \cdot \langle u' \otimes u' \rangle = 0, \qquad \nabla \cdot u = 0. \tag{14}$$

The quantity

$$R = \langle u' \otimes u' \rangle \tag{15}$$

is called the Reynolds tensor.

It is reasonable (Reynolds' hypothesis) to relate R to $\nabla u + \nabla u^{\mathrm{T}}$ because turbulence occurs in places where ∇u is large (with a few exceptions such as boundary layers before transition and turbulence in decay). It was shown in Reference 7 that with Reynolds' hypothesis the only possible form for R compatible with reference frame invariance of (14) is

$$R = aI + b(\nabla u + \nabla u^{\mathrm{T}}) \quad \text{in 2D}, \tag{16}$$

$$R = aI + b(\nabla u + \nabla u^{\mathrm{T}}) + c(\nabla u + \nabla u^{\mathrm{T}})^2 \quad \text{in 3D}, \tag{17}$$

where a, b and c are functions of the invariants of $\nabla u + \nabla u^{\mathrm{T}}$ only. Since $\nabla \cdot u = 0$, there are only two such invariants in 3D, $|\nabla u + \nabla u^{\mathrm{T}}|$ and $\det(\nabla u + \nabla u^{\mathrm{T}})$, and only one in 2D, $|\nabla u + \nabla u^{\mathrm{T}}|$.

Now R appears only through $\nabla \cdot R$ in (14) and $\nabla \cdot (aI)$ is a pressure term ∇a so (16) is functionally equivalent in 2D to (b is now denoted by ν_{T})

$$\nabla \cdot R = \nabla \cdot [\nu_{\mathrm{T}}(\nabla u + \nabla u^{\mathrm{T}})], \tag{18}$$

where ν_{T} is any function of $|\nabla u + \nabla u^{\mathrm{T}}|$.

In Smagorinsky's model[8] ν_{T} is chosen proportional to $|\nabla u + \nabla u^{\mathrm{T}}|$:

$$R = -ch^2 |\nabla u + \nabla u^{\mathrm{T}}| (\nabla u + \nabla u^{\mathrm{T}}), \qquad c = 0{\cdot}01. \tag{19}$$

The fact that ν_{T} is a function of h is based on an ergotic hypothesis which replaces the expected value by a space averaging; if this is allowed then w in (11) tends to zero with h since it represents the part of the flow which is not computable because it falls under the grid (subgrid-scale modelling; see e.g. Reference 9). The power 'two' in h^2 in (19) is found from a dimensionality argument.

Deardorff,[10] Moin and Kim,[11] Horiuti[12] and Schumann[13] were able to reproduce turbulent channel flows quite accurately with this model. However, for flows around obstacles we have been less successful; it seems that the model is adequate only if there are already a sufficient number of grid points to represent the beginning of the Kolmogorov range of the flow. Notice also that (19) is unlikely in 3D since the general form (17) must be considered in principle. A similar suggestion can be found in References 14 and 15.

2.2. *The k–ε model*

A more elaborate model was proposed by Launder and Spalding[16] and Rodi[17]: the so-called k–ε model.

Set k as the turbulent kinetic energy and ε as the turbulent rate of dissipated energy, so

$$k = \tfrac{1}{2} \langle |u'|^2 \rangle, \tag{20}$$

$$\varepsilon = \frac{\nu}{2} \langle |\nabla u' + \nabla u'^{\mathrm{T}}|^2 \rangle, \tag{21}$$

$$R = \tfrac{2}{3} kI - c_\mu \frac{k^2}{\varepsilon} (\nabla u + \nabla u^{\mathrm{T}}), \tag{22}$$

$$k_{,t}+u\nabla k-\frac{c_\mu}{2}\frac{k^2}{\varepsilon}|\nabla u+\nabla u^{\mathrm{T}}|^2-\nabla\cdot\left(c_\mu\frac{k^2}{\varepsilon}\nabla k\right)+\varepsilon=0, \tag{23}$$

$$\varepsilon_{,t}+u\nabla\varepsilon-\frac{c_1}{2}k|\nabla u+\nabla u^{\mathrm{T}}|^2-\nabla\cdot\left(c_\varepsilon\frac{k^2}{\varepsilon}\nabla\varepsilon\right)+c_2\frac{\varepsilon^2}{k}=0, \tag{24}$$

with $c_\mu=0{\cdot}09$, $c_1=0{\cdot}1296$, $c_2=1{\cdot}92$ and $c_\varepsilon=0{\cdot}07$.

Natural boundary conditions could be

$$k,\varepsilon \text{ given at } t=0, \qquad k|_\Gamma=k_\Gamma, \qquad \varepsilon|_\Gamma=\varepsilon_\Gamma. \tag{25}$$

However, an attempt can be made to remove the low-Reynolds-number regions from the computational domain by considering 'wall conditions'

$$k|_\Gamma=u^{*2}c_\mu^{-1/2}, \qquad \varepsilon|_\Gamma=u^{*3}/\kappa\delta, \tag{26}$$

$$u\cdot n=0, \qquad \alpha u\cdot\tau+\beta\,\partial u\cdot\tau/\partial n=\gamma, \tag{27}$$

where κ is the Von Karman constant ($\kappa=0{\cdot}41$), δ is the boundary layer thickness, u^* (computed by (28)) is the friction velocity, $\beta=c_\mu k^2/\varepsilon$, $\alpha=\beta/\{\kappa\delta[B+\kappa^{-1}\log(\delta/D)]\}$ (where D is a roughness constant), $\gamma=-u^*|u^*|$ and B is such that (27) matches with the viscous sublayer. To compute u^*, Reichard's law may be used:

$$u^*=\frac{u\cdot\tau}{f(u^*)}; \qquad f(u^*)=2{\cdot}5\log(1+0{\cdot}4y^+)+7{\cdot}8\left(1-\mathrm{e}^{-y^+/11}-\frac{y^+}{11}\mathrm{e}^{-0{\cdot}33y^+}\right), \tag{28}$$

with $y^+=\delta u^*/\nu$. Thus in reality α, β and γ in (27) are non-linear functions of $u\cdot\tau$. For smooth walls it is suggested to take $\alpha=\gamma=0$.

For physical and mathematical reasons it is essential that the system (20)–(24) yields positive values for k and ε. At least in some cases it is possible to argue that if the system has a smooth solution for given positive initial data and zero Dirichlet conditions on the boundaries, then k and ε stay positive at later times. For this purpose one looks at

$$\theta=k/\varepsilon.$$

If D_t denotes the total derivative operator, $\partial/\partial t+u\nabla$ and E denotes $\frac{1}{2}|\nabla u+\nabla u^{\mathrm{T}}|^2$, then

$$\begin{aligned}
D_t\theta&=\frac{1}{\varepsilon}D_tk-\frac{k}{\varepsilon^2}D_t\varepsilon\\
&=\theta^2E(c_\mu-c_1)+\frac{c_\mu}{\varepsilon}\nabla\cdot\frac{k^2}{\varepsilon}\nabla k-c_\varepsilon\frac{k}{\varepsilon^2}\nabla\cdot\frac{k^2}{\varepsilon}\nabla\varepsilon-1+c_2\\
&=\theta^2E(c_\mu-c_1)-1+c_2+c_\mu\nabla\cdot\frac{k^2}{\varepsilon}\nabla\theta+2c_\mu\theta^2\nabla\theta\cdot\nabla\left(\frac{k}{\theta}\right)+(c_\mu-c_\varepsilon)\frac{k}{\varepsilon^2}\nabla\cdot\frac{k^2}{\varepsilon}\nabla\varepsilon.
\end{aligned}$$

In this equation it is seen that because $c_\mu<c_1$ and $c_2>1$, θ will stay positive and bounded when there are no diffusion terms. Indeed, the equation then reduces to

$$D_t\theta=\theta^2E(c_\mu-c_1)-1+c_2,$$

whose solution is always bounded when ε is constant.

Also, θ cannot become negative even in the presence of viscous terms if $c_\mu=c_\varepsilon$, because the moment the minimum of θ is zero at (x, t) we will have

$$\nabla\theta=0, \qquad \theta=0;$$

so at this point we get

$$\theta_{,t} - c_2 + 1 = 0,$$

which is impossible because θ cannot become negative unless $\theta_{,t} \leqslant 0$.

In Reference 18 a q–f formulation is described, where $q = k^{1/2}$ and f is the frequency of the large-scale motions, whose numerical performance is appreciably better than the first one. In a similar fashion, in Reference 19 a k–θ model with $\theta = k/\varepsilon$ is presented and numerical results are compared with the results obtained with the k–ε model.

2.3. *A k–ε model with memory*

In Reference 20 an attempt was made to prove Reynolds' hypothesis (18) by assuming that the turbulent part of the flow has a length scale l much smaller than the length scale L of the mean flow. With $\eta = l/L$ it was shown (see also Reference 21) that the solution u^ε of the problem

$$u^\eta_{,t} + (u^\eta \cdot \nabla)u^\eta + \nabla p^\eta - \mu\eta^2 \Delta u^\eta = 0, \qquad \nabla \cdot u^\varepsilon = 0 \quad \text{in} \quad \Omega \times]0, T[,$$

$$u^\eta(x, 0) = u^0(x) + \eta^{1/3} w^0(x/\eta, x) \tag{29}$$

converges to the solution of ($n = 2$ in 2D, $n = 3$ in 3D)

$$u_{,t} + (u \cdot \nabla)u + \nabla p + \nabla \cdot \left(q^0(a(x,t)) \frac{\beta_0}{(1+i)^2} \, e^{-\mu\gamma_0 t(x)} \, e^{2\beta_0/(d+1) - 2\beta_0/(1+i)} \nabla a \nabla a^{\mathrm{T}} \right) = 0, \tag{30}$$

$$\nabla \cdot u = 0, \tag{31}$$

where a is the inverse Lagrangian co-ordinate, i.e. the solution of

$$a_{,t} + u\nabla a = 0, \qquad a(x, 0) = x, \qquad a|_{\Gamma_{\mathrm{in}}} = x - ut \tag{32}$$

(where Γ_{in} is the inflow boundary), $\beta_0 = 1/3$ and

$$i = \sum_{l,j} a^2_{l,j}, \qquad t(x) = \min\{t, t - s : a(x, s) \in \Gamma, s \geqslant 0\}. \tag{33}$$

This model is referred to below as the MPP model.

In (30) the stress tensor is not viscous in the sense that it conserves energy when $\mu = 0$:

$$\int_\Omega (\tfrac{1}{2}u^2 + q^0(a(x,t)\, e^{2\beta_0/(n+1) - 2\beta_0/(1+i)}) \, dx = \text{constant}. \tag{34}$$

To account for dissipation one must pursue further the asymptotic expansion that led to (30); then a term proportional to $q^{1/2}(\nabla u + \nabla u^{\mathrm{T}})$ is found and the model becomes

$$u_{,t} + (u \cdot \nabla)u + \nabla p + \nabla \cdot \left(\frac{\beta_0 q}{(1+i)^2} \nabla a \nabla a^{\mathrm{T}} - \nu_0 q^{1/2}(\nabla u + \nabla u^{\mathrm{T}}) \right) = 0, \tag{35}$$

where

$$q = q^0(a(x,t)) \, e^{-\mu\gamma_0 t(x)} \, e^{2\beta_0/(n+1) - 2\beta_0/(1+i)}, \tag{36}$$

with $\gamma_0 = 1/9$. However, it was found in Reference 19 that this is too crude a model for the viscous effect of the turbulence. Since the k–ε model is quite good at simulating the effect of dissipation, we also built a mixed model where the kinetic turbulent energy is the product of that coming from the MPP model and that coming from the k–ε model; and similarly, the rate of dissipated turbulent energy is the product of the kinetic energy of the MPP model and ε found in the k–ε

model. The Reynolds tensor is the sum of the tensors of both models:

$$R = k\frac{\beta_0 e^{2\beta_0/(n+1)-2\beta_0/(1+i)}}{(1+i)^2}\nabla a\nabla a^{\mathrm{T}} - c_\mu q\frac{k^2}{\varepsilon}(\nabla u+\nabla u^{\mathrm{T}}), \tag{37}$$

$$k_{,t}+u\nabla k-\frac{c_\mu}{2}\frac{k^2}{\varepsilon}|\nabla u+\nabla u^{\mathrm{T}}|^2-\nabla\cdot\left(c_\mu\frac{k^2}{\varepsilon}\nabla k\right)+\varepsilon=0, \tag{38}$$

$$\varepsilon_{,t}+u\nabla\varepsilon-\frac{c_1}{2}k|\nabla u+\nabla u^{\mathrm{T}}|^2-\nabla\cdot\left(c_\varepsilon\frac{k^2}{\varepsilon}\nabla\varepsilon\right)+c_2\frac{\varepsilon^2}{k}=0, \tag{39}$$

$$i=\sum_{l,j}a_{l,j}^2, \tag{40}$$

$$a_{,t}+u\nabla a=0, \qquad a(x,0)=x. \tag{41}$$

Notice that by changing the value of the constants we can pass continuously from the k–ε model to the MPP model.

3. DISCRETIZATION BY FEM AND CHARACTERISTICS

Total derivative discretization was introduced simultaneously by Ukeguchi *et al.*,[22] Douglas and Russell,[23] Benqué *et al.*[24] and Pironneau.[25]

If $\chi_h^n(x)$ denotes an approximation to $\chi(n\delta t)$, the solution at $\lambda=n\delta t$ of

$$\mathrm{d}\chi/\mathrm{d}\lambda=u(\chi(\lambda),\lambda), \qquad \chi((n+1)\delta t)=x, \tag{42}$$

then (5), (7) is discretized in time by

$$\begin{aligned}&([u_h^{n+1}-u_h^n\circ\chi_h^n]\delta t^{-1},v_h)+(\nu\nabla u_h^{n+1},\nabla v_h)=(f^n,v_h),\\ &\forall v_h\in J_{0h}, \qquad u_h^{n+1}-u_{\Gamma h}\in J_{0h}.\end{aligned} \tag{43}$$

With turbulence modelling, ν and f may be functions of x, ∇u^n, k^n, ε^n, etc.

Because of the constraints on the divergence of v_h in J_{0h}, (43) is a linear system of the type

$$Av+BP=F, \qquad B^{\mathrm{T}}V=0, \tag{44}$$

where P represents the Lagrange multipliers of the constraints (but also an approximation of the pressure at the vertices). V can be formally eliminated:

$$B^{\mathrm{T}}A^{-1}BP=B^{\mathrm{T}}A^{-1}F, \tag{45}$$

but this system being symmetric positive semidefinite, it can be solved by a preconditioned conjugate gradient algorithm as explained in References 26 and 27; the only difference is that here A is a function of $t=n\delta t$ through ν_{T}.

In principle, the same time discretization scheme can be applied to the remaining equations of the turbulent model.

In the case of the Lagrangian co-ordinate $a(x,t)$ we found that it is better to integrate ∇a directly and use the identity $\det\nabla a=1$ to reduce the number of equations:

$$(a_h^{n+1},v_h)=(a_h^n\circ\chi_h^n,v_h), \quad \forall v_h\in V_h, \tag{46}$$

$$(a_{h,j}^{n+1},v_h)=(a_{h,j}^n\circ\chi_h^n,v_h)-\sum_i\delta t(u_{,i}\,a_{h,i}^n), \quad j=1,\ldots,n. \tag{47}$$

For the k–ε equations the algorithm is extremely sensitive to the discretization scheme because of the negative sign in the production terms. After several months of effort to find a stable scheme for transient flows, we arrived at the following.

As in Reference 28, the equation for k is discretized by

$$(k_h^{n+1}, v_h)+\delta t c_\mu\left(\frac{k_h^{n2}}{\varepsilon_h^n}\nabla k_h^{n+1}, \nabla w_h\right)=(k_h^n\circ\chi_h^n, v_h)+\left(\int_{]x,\chi_h^n(x)[}\left(\frac{c_\mu}{2}\frac{k_h^{n2}}{\varepsilon_h^n}|\nabla u_h^n+\nabla u_h^{n\mathrm{T}}|^2-\varepsilon_h^n\right), w_h\right), \tag{48}$$

$$\forall w_h\in Q_{0h}=\{w_h\in Q_h: w_h|_\Gamma=0\}, \qquad k_h-k_{\Gamma h}\in Q_{0h}. \tag{49}$$

The equation for ε is treated in two steps via a convection of $\theta=k/\varepsilon$. Without diffusion, θ satisfies

$$\theta_{,t}+u\nabla\theta+c_\mu\frac{\theta^2}{2}|\nabla u+\nabla u^{\mathrm{T}}|^2=c_2-1. \tag{50}$$

Thus a convection step on θ that does not include the viscous terms is

$$(\theta_h^{n+1/2}, w_h)+\left(\theta_h^{n+1/2}\int_{]\chi_h^n(x),\, x[}\left(\frac{\theta_h^n}{2}|\nabla u_h^n+\nabla u_h^{n\mathrm{T}}|^2(c_1-c_\mu)\right), w_h\right)=(\theta_h^n\circ\chi_h^n, w_h)+(c_2-1, w_h)\delta t, \tag{51}$$

where $\theta_h^n=k_h^n/\varepsilon_h^n$. Then $\varepsilon_h^{n+1/2}$ is found as

$$\varepsilon_h^{n+1/2}=\frac{k_h^{n+1}}{\theta_h^{n+1/2}} \tag{52}$$

and a diffusion step can be applied to find ε_h^{n+1}:

$$(\varepsilon_h^{n+1}, w_h)+\delta t c_\varepsilon\left(\frac{k_h^{n2}}{\varepsilon_h^n}\nabla\varepsilon_h^{n+1}, \nabla w_h\right)=(\varepsilon_h^{n+1/2}, w_h), \tag{53}$$

$$\forall w_h\in Q_{0h}, \qquad \varepsilon_h^{n+1}-\varepsilon_{\Gamma h}\in Q_{0h}. \tag{54}$$

Notice that this scheme is not likely to produce negative values for k_h^{n+1} and ε_h^{n+1} because $c_1>c_\mu$ and $c_2>1$.

To improve the stability it is possible to replace (48) by

$$(k_h^{n+1}, v_h)+\left(k_h^{n+1}\int_{]\chi_h^n(x),\, x[}\frac{\theta_h^n}{2}|\nabla u_h^n+\nabla u_h^{n\mathrm{T}}|^2 c_\mu, w_h\right)+\delta t c_\mu\left(\frac{k_h^{n2}}{\varepsilon_h^n}\nabla k_h^{n+1}, \nabla w_h\right)$$
$$=(k_h^n\circ\chi_h^n, v_h)-\left(\left(\int_{]x,\chi_h^n(x)[}\varepsilon_h^n\right), w_h\right),$$

$$\forall w_h\in Q_{0h}=\{w_h\in Q_h: w_h|_\Gamma=0\}, \qquad k_h-k_{\Gamma h}\in Q_{0h}.$$

Note also that (52) should be implemented weakly, e.g.

$$(\varepsilon_h^{n+1/2}, w_h)=(k_h^{n+1/2}/\theta_h^{n+1/2}, w_h) \quad \forall w_h\in Q_h.$$

This procedure may induce negative $\varepsilon_h^{n+1/2}$ if $k_h^{n+1/2}/\theta_h^{n+1/2}$ is too irregular.

4. BOUNDARY CONDITIONS

The boundary conditions for k_h and ε_h are standard Dirichlet conditions but the boundary conditions for u_h (see (30)) are non-linear Robin-type for $u_h\cdot\tau$ and Dirichlet-type for $u_h\cdot n$. Since

each time step of the algorithm requires the solution of a generalized Stokes problem (see (42)), we can discuss the implementation of these conditions on the Stokes problem only:

$$\alpha u - \nabla \cdot \nu_T(\nabla u + \nabla u^T) + \nabla p = g, \qquad \nabla \cdot u = 0 \quad \text{in} \quad \Omega, \tag{55}$$

$$u \cdot n = 0, \qquad au \cdot \tau + \nu_T \frac{\partial u}{\partial n} \cdot \tau = 0 \quad \text{on} \quad \Gamma. \tag{56}$$

A variational formulation is ($d=2$ or 3)

$$\alpha(u, v) + (\nu_T(\nabla u + \nabla u^T), \nabla v) + \int_\Gamma au \cdot v = (g, v), \quad \forall v \in J_{0h}(\Omega), \tag{57}$$

$$u \in J_{0h}(\Omega) = \{v \in H^1(\Omega)^d : \nabla \cdot v = 0, v \cdot n|_\Gamma = 0\}. \tag{58}$$

This can be discretized as before by

$$\alpha(u_h, v_h) + (\nu_T(\nabla u_h + \nabla u_h^T), \nabla v_h) + \int_{\Gamma_h} au_h \cdot v_h = (g, v_h), \quad \forall v_h \in J_{0nh}, \tag{59}$$

$$u_h \in J_{0nh} = \{v_h \in V_h : (\nabla \cdot v_h, q_h) = 0, \forall q_h \in Q_h, v_h \cdot n_h|_\Gamma = 0\}, \tag{60}$$

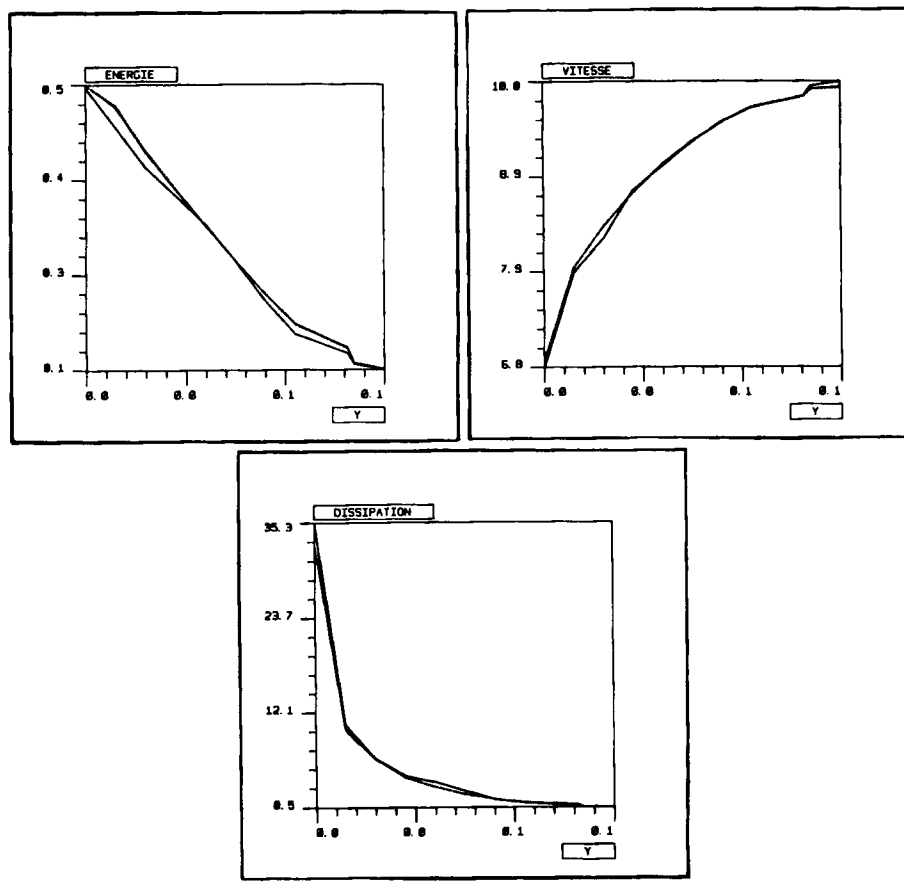

Figure 1. —— Initial, ... k–ε, – – – – – mixed model.

where $n_h(x^j)$ is an approximation of n at the nodes $\{x^j\}$ of the triangulation for u_h. Although this works well (some of the results at the end have been obtained with this method), it is not easy to choose n_h in a way that differentiates between real corners or edges of Ω and corners or edges of Ω_h which are due to the piecewise linear approximation of Γ by Γ_h.

A nice trick, although less precise, is to notice that if u, q are in H^1,

$$(u, \nabla q)=0, \quad \forall q \Leftrightarrow \nabla \cdot u=0 \quad \text{in } \Omega \quad \text{and} \quad u \cdot n=0 \quad \text{on } \Gamma, \tag{61}$$

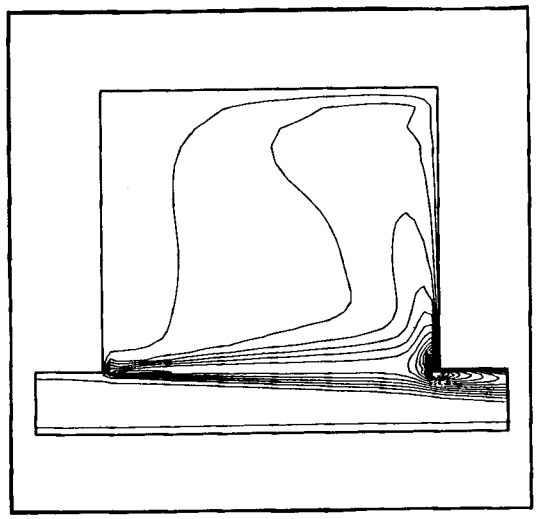

Figure 2.

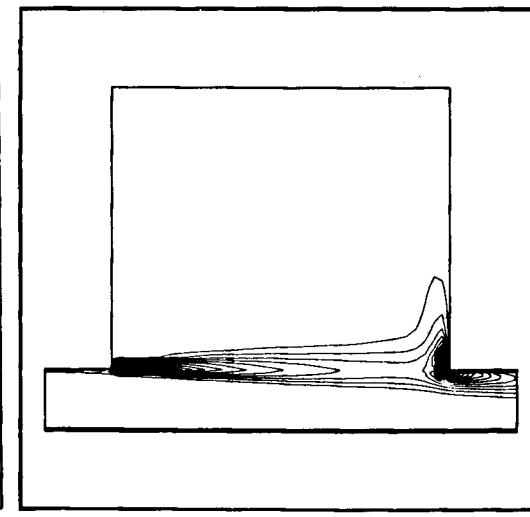

Figure 3.

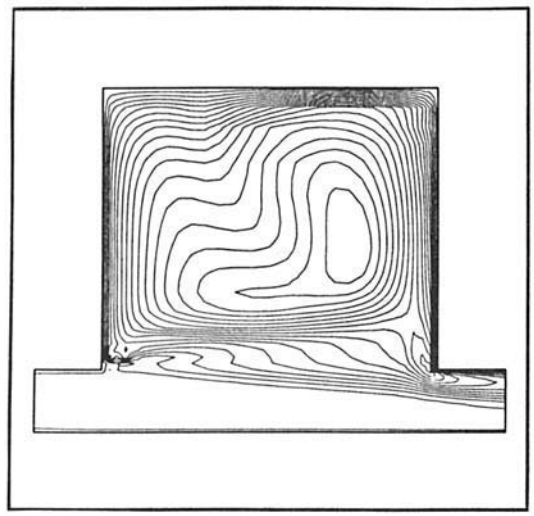

Figure 4.

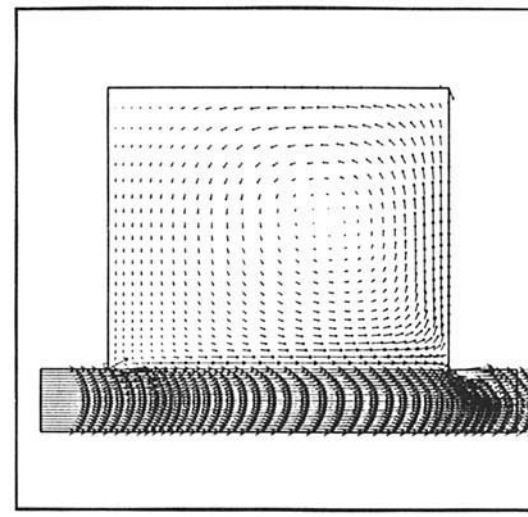

Figure 5.

because

$$\int_\Omega u\nabla q = -\int_\Omega q\nabla\cdot u + \int_\Gamma u\cdot nq. \tag{62}$$

Thus another discretization for (55), (56) is

$$J'_{0nh} = \{v_h \in V_h : (v_h, \nabla q_h) = 0, \forall q_h \in Q_h\}. \tag{63}$$

Parès[29] showed that the solution of (57), (61) converges to the solution of (55), (56) with an H^1-error $O(\sqrt{h})$; thus although (63) is much easier to implement, one loses some precision.

For the outflow boundary Γ_{out} several options were tested: Neumann conditions for (53),

$$\alpha u - \nu_T \nabla u\cdot n + pn = 0; \tag{64}$$

no stress,

$$\nu_T(\nabla u + \nabla u^T)\cdot n - pn = 0; \tag{65}$$

no tangential stress,

$$u\cdot n = u_\infty \cdot n, \qquad \alpha u\cdot\tau - \nu_T(\partial u/\partial n)\tau = 0; \tag{66}$$

free convection,

$$u^{n+1} - u^n \circ \chi^n = 0; \tag{67}$$

condition on the pressure,

$$p = p_\infty, \qquad u \wedge n = r, \tag{68}$$

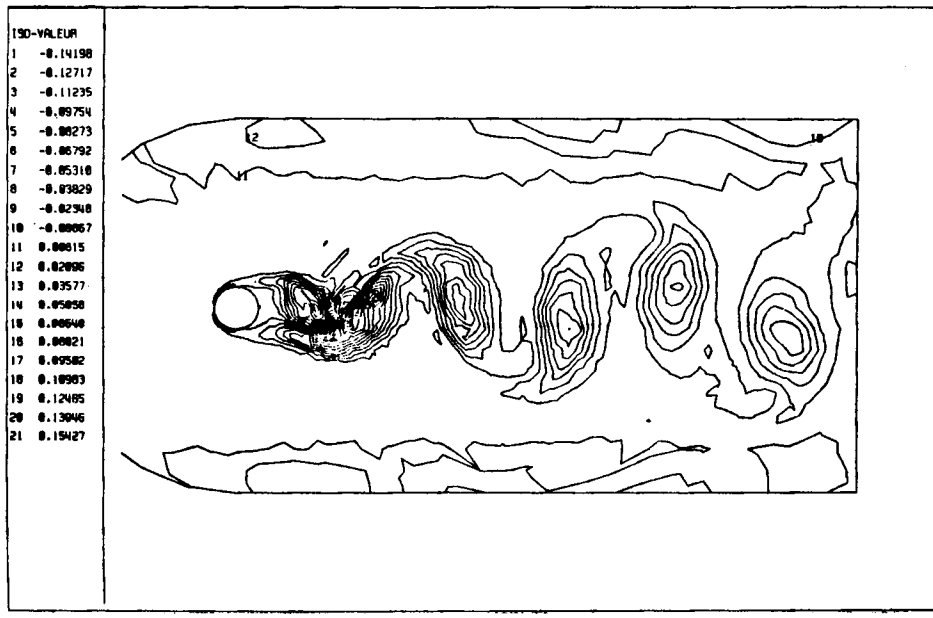

Figure 6.

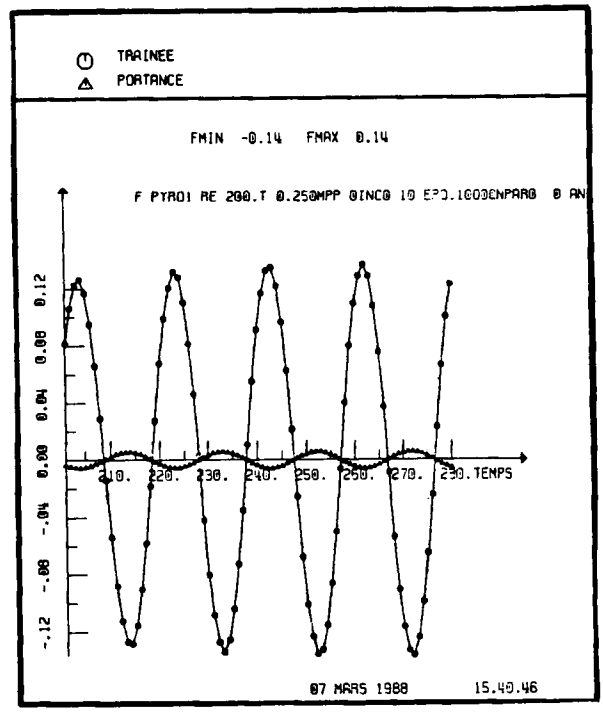

Figure 7.

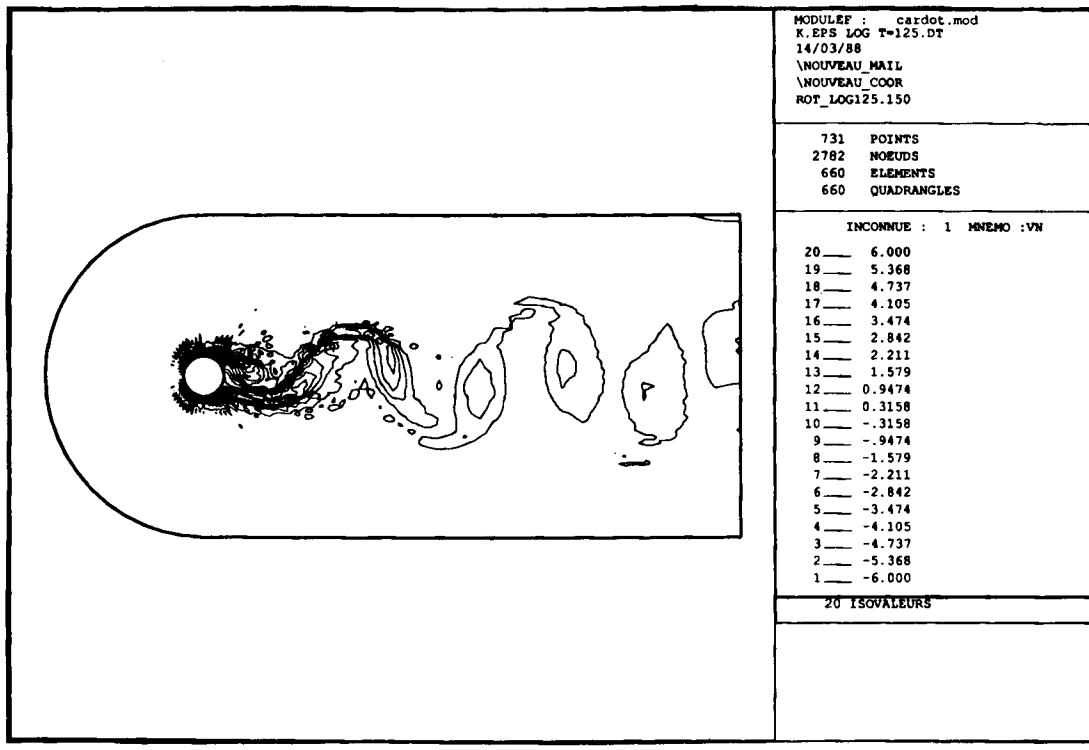

Figure 8.

where $r=0$ or $r=u^n \circ \chi^n$. This last condition is implemented by replacing (43) by (69)

$$\alpha(u_h, v_h)+\nu(\nabla \wedge u_h, \nabla \wedge v_h)+\nu(\nabla \cdot u_h, \nabla \cdot v_h)=(f, v_h)+\int_{\Gamma_\infty} p_\infty n_h \cdot v_h, \tag{69}$$

$$v_h, u_h \in J''_{0h}=\{v_h \in V_h : (\nabla \cdot v_h, q_h)=0, \forall q_h \in Q_h; v_h \wedge n_h=0\}; \tag{70}$$

see References 4 and 30–32 for further details.

5. NUMERICAL RESULTS

5.1. *Plane Poiseuille flow with the k–ε model*

The domain is rectangular and 2D. The inflow conditions on u_h, k_h and ε_h are taken from the experiment of Comte-Bellot;[33] Neumann conditions are given at the outflow. The k–ε logarithmic wall laws are used on the horizontal walls, with $Re=57000$. Figure 1 displays k, ε and u_1 and shows good agreement with other similar computations[34] and with the mixed MPP/k–ε model. Notice that in this case of stationary mean flow there are not many differences between the k–ε model and the mixed model; the memory term $R(\nabla a)$ vanishes.

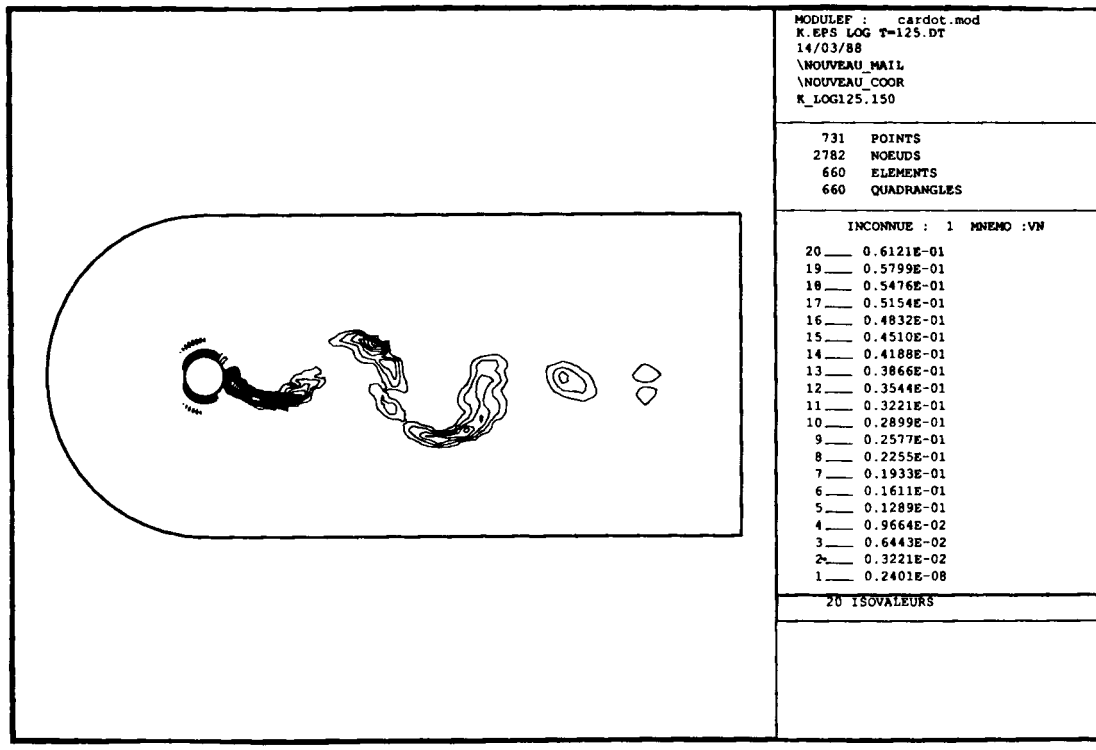

Figure 9.

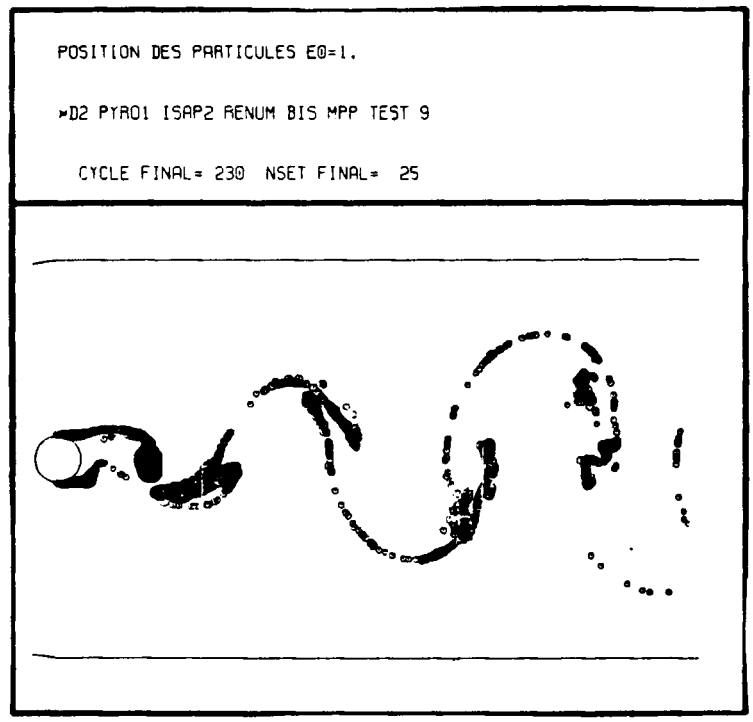

Figure 10.

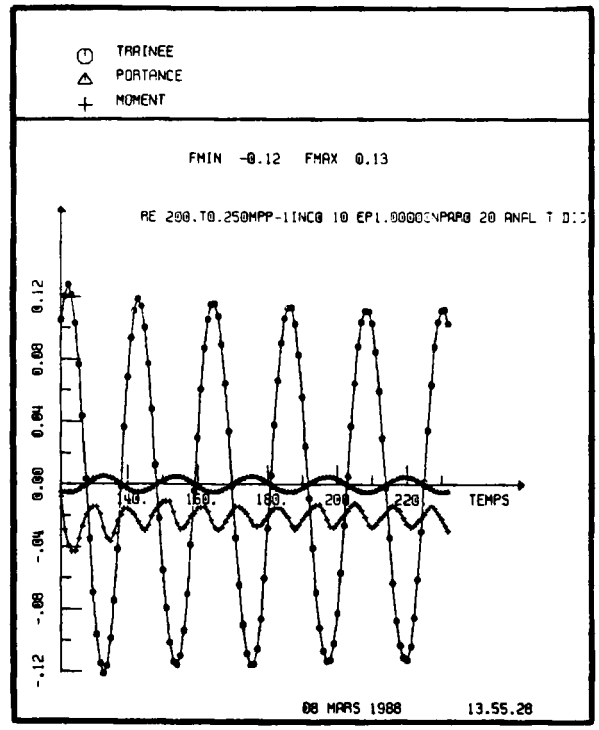

Figure 11.

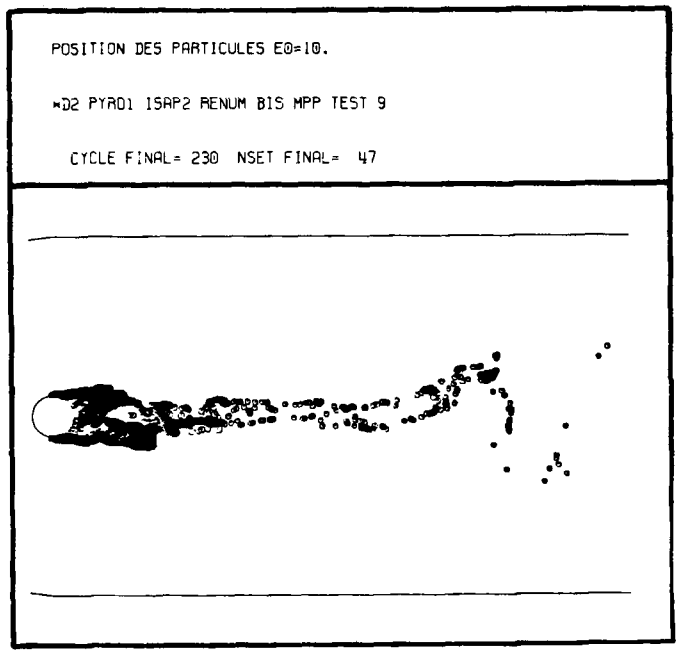

Figure 12.

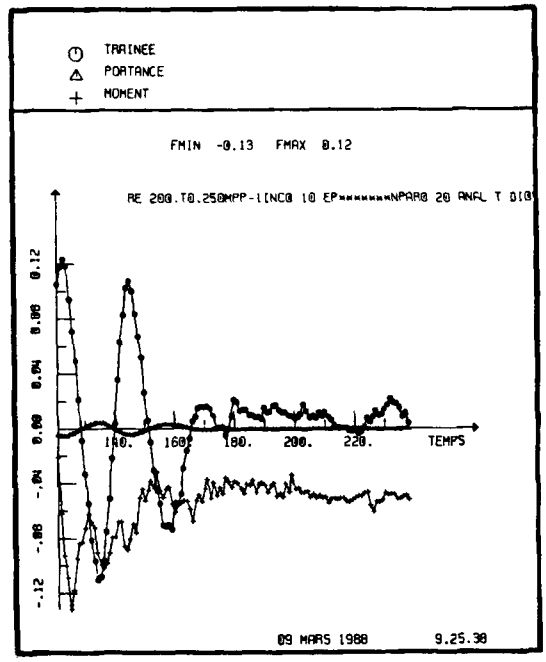

Figure 13.

5.2. *Flow in a cavity with the k–ε model*

Similar conditions to those of Section 5.1 are imposed on the inflow and outflow boundaries and on the walls, with $Re = 100000$. The computed flow is stationary and the figures display k (Figure 2), ε (Figure 3), ν_T (Figure 4) and u (Figure 5).

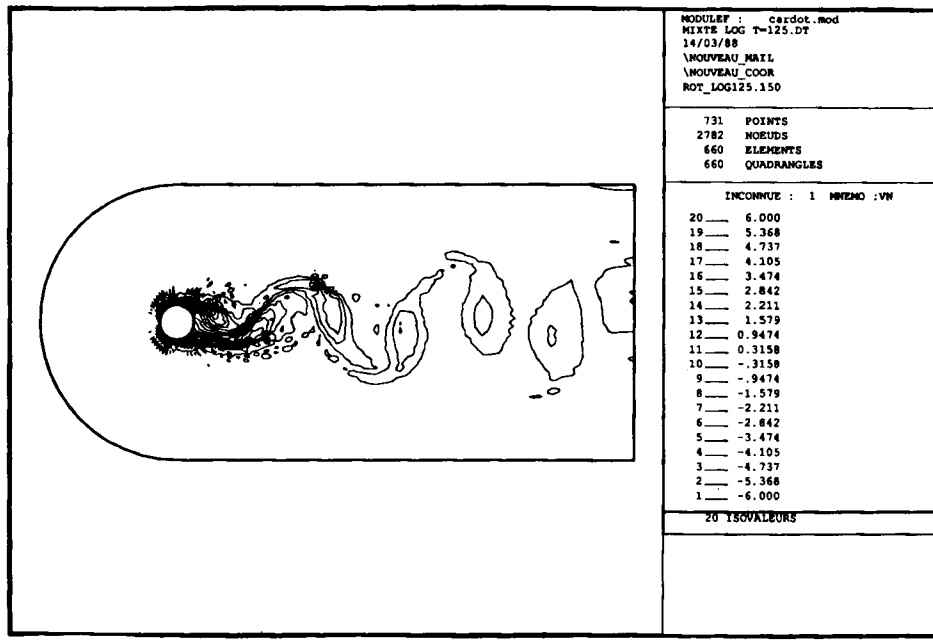

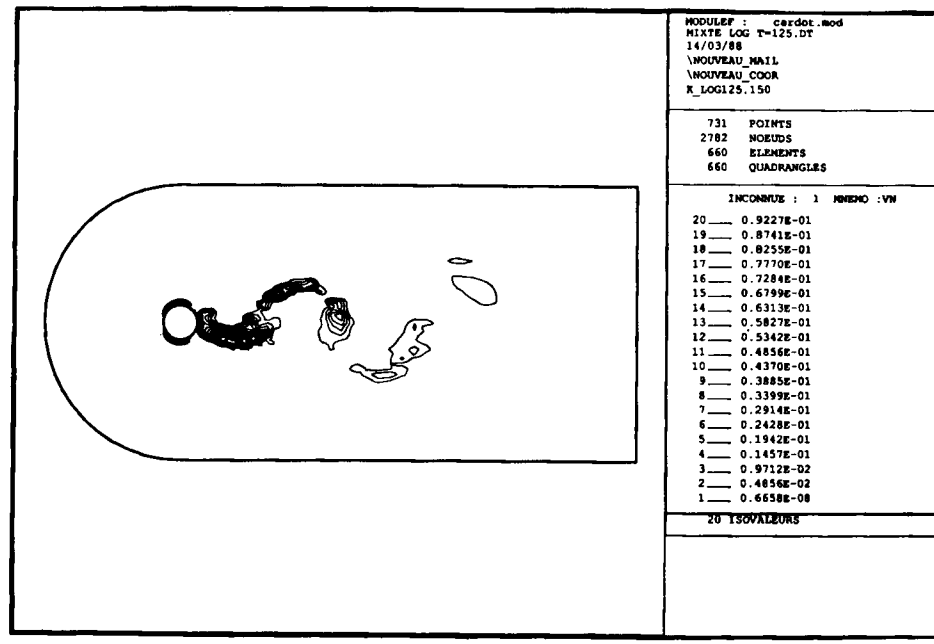

Figure 14.

5.3. Flow behind a cylinder without turbulence model

A direct simulation of the Navier–Stokes equations with $Re=200$ is made. The figures show $\nabla \wedge u$ (Figure 6) at different instants and the drag–lift (Figure 7) and moment on the cylinder as a function of time.

5.4. Flow behind a cylinder with the k–ε model at $Re=500$

Starting from the results of Section 5.3, the k–ε model is activated into the Navier–Stokes equation with $k=\varepsilon=10^{-7}$ at inflow and outflow boundaries. The figures show $\nabla \wedge u$ (Figure 8) and k (Figure 9) at $t=30$ s. Reichard's wall law has been used. Simulation at $Re=10000$ with a k–k/ε model have also been carried out.[35]

5.5. Flow behind a cylinder with the MPP model at $Re=200$

A similar computation is made with the MPP model with $q|_\Gamma=0{\cdot}1$ and 10 on two triangles near the region where the boundary layer separates and $q|_\Gamma=0$ elsewhere. The discretization for q uses a particle method, more appropriate to this type of boundary conditions. The results show, for $q|_\Gamma=0{\cdot}1$, q (Figure 10) and the drag-lift (Figure 11), and for $q|_\Gamma=10$, ∇q (Figure 12) at $t=30$ s and the drag–lift and moment on the cylinder (Figure 13).

5.6. Flow behind a cylinder with the mixed MPP/k–ε model

This is the same as in Section 5.4 but with $k^0=0$, $q|_\Gamma=0{\cdot}1$ at the separation points and k_Γ, ε_Γ as in Section 5.4 elsewhere.

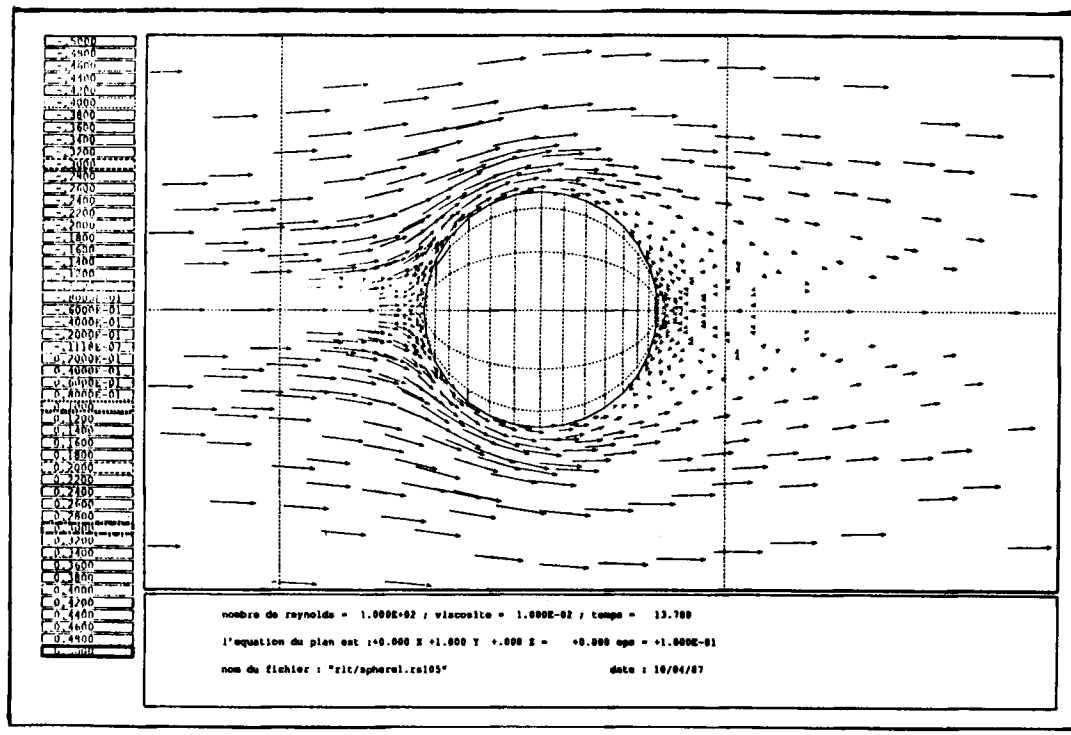

Figure 15.

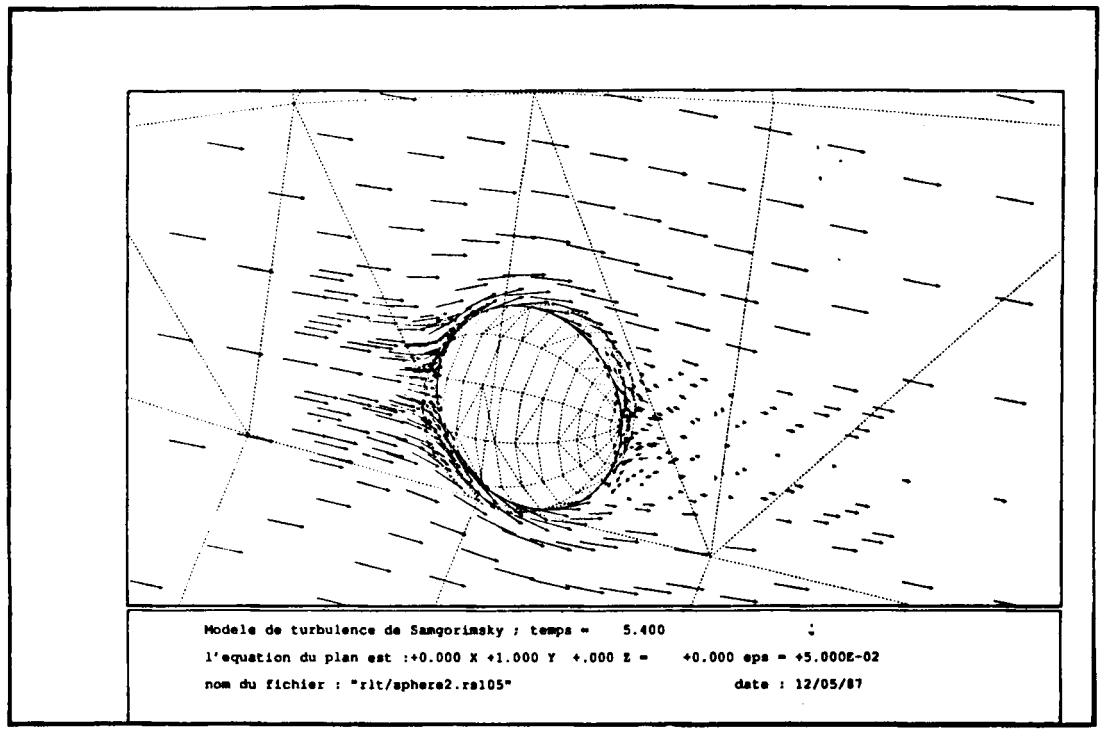

Figure 16.

5.7. *Flow behind a sphere*

To evaluate the influence of the outflow condition, simulations with (62), (63), (64) or (65) were made at $Re = 1000$ with the Navier–Stokes equation without turbulence modelling. A direct simulation at $Re = 100$ was made with the no-slip boundary condition imposed weakly (Figure 15) and a computation with the Smagorinsky eddy viscosity was also made together with the wall laws (Figure 16). With the grid used the flow is steady.

6. DISCUSSION AND CONCLUSIONS

One major criticism Speziale[15] made of the k–ε model is its inability to predict secondary eddies in 3D in certain configurations. This may be due to the missing term ($c = 0$ in (16)). However, in 2D the model is both consistent with Reynolds' hypothesis and frame-independent as shown at the beginning. The main conclusion of this study and our numerical tests is that the model does not always yield stationary solutions.

Several researchers known to the authors have attempted a simulation of the flow behind a cylinder with the k–ε model without success, the main difficulty being that classical algorithms (explicit or Newton steps) fail to converge or that they generate negative values for k or ε. We have shown in this paper that by carefully studying the positivity of the variables it is possible to construct semi-implicit, second-order in time, L^2-stable algorithms. Our algorithm is sufficiently robust to yield a solution to the difficult problem of simulating the flow behind a cylinder with the k–ε model; it also produces the known answers on problems such as pipe flow or cavity flow. However, our study raises a major question: is the solution stationary or transient?

From a theoretical point of view it is almost certain that both solutions exist, as for the Navier–Stokes equations without turbulence modelling. So the real question is the stability of the stationary solution. Suppose that by other methods one is able to compute a stationary solution of the model; if the solution is unstable then any small perturbation will induce a bifurcation towards the transient solution. Then, is there any value in a turbulence model that produces unstable solutions? The authors believe that the answer is no and that the transient solution is more interesting physically.

Quite a number of authors derive the k–ε model by taking time averages of the fluctuating quantities. Of course the mean flow cannot be transient then unless there are two time scales in the flow and the averaging process applies to the small time scale. But since it is equally easy to derive the k–ε model by taking ensemble averages over fluctuating initial data, one can construct a time-dependent model also.

As pointed out by Rodi (private communication), the very fact that one computes a 2D solution of a flow which has 3D fluctuations implies an ensemble or space-averaging process.

The next question is the connection between the k–ε model and a Eulerian–Lagrangian model (MPP) which is similar except for a term which involves the Lagrangian co-ordinate of the flow. This model was derived with some mathematical rigour in Reference 20 for flows which have two well-separated scales (such as the flow right behind the cylinder). The model is difficult to implement because it is numerically unstable without dissipation terms and too dissipative otherwise. But in this paper we have recalled that both models are in fact complementary and that one can build a k–ε model with memory by mixing the two. However, our numerical simulations show that the viscous effects dominate the memory effect and that the results produced are not very different for the type of mesh used here.

Much still remains to be done before drawing hard conclusions. We would have liked to try several meshes and several time-stepping procedures to check the independence of the solutions on these, but our computing means (20 h of CRAY 2) did not allow us to proceed further for the time being. Comparison of the two models and analysis of the results are difficult for us numerical analysts.

The point is that our task is not to discuss the validity of the model from the point of view of fluid mechanics but to show to the physicist what the consequences of his model are. The present study, for instance, shows that it is not reasonable to expect a stationary solution to the k–ε model because the viscosity created by the model is not sufficient to stabilize the stationary flow.

REFERENCES

1. J. L. Lions, *Quelques Methodes de Resolution des Problèmes aux Limites Nonlineaires*, Dunod, Paris, 1968.
2. O. Ladyzhenskaya, *The Mathematical Theory of Viscous Incompressible Flows*, Gordon and Breach, London, 1963.
3. F. Thomasset, *Implementation of Finite Element Methods for Navier–Stokes Equations, Springer series in Computational Physics, Vol. 12*, Springer, Berlin, 1981.
4. O. Pironneau, *Finite Element Methods for Fluids*, Wiley, New York, 1989.
5. D. Arnold, F. Brezzi and M. Fortin, 'A stable finite element for the Stokes equations', *Calcolo*, **21**, 337–344 (1984).
6. C. Bernardi and G. Raugel, 'A conforming finite element method for the time-dependent Navier–Stokes equations', *SIAM J. Numer. Anal.*, **22**, 455–473 (1985).
7. T. Chacon and O. Pironneau, 'On the mathematical foundations of the k–ε model', in A. V. Balakrishnan (ed.), *Vistas in Applied Mathematics*, Optimization Software Inc., Springer, New York, 1986, pp. 44–56.
8. J. S. Smagorinsky, 'General circulation model of the atmosphere', *Mon. Weather Rev.*, **91**, 99–164 (1963).
9. M. Lesieur, *Turbulence in Fluids*, Martinus Nijhoff, Dordrecht, 1987.
10. J. W. Deardorff, 'A numerical study of 3-d turbulent channel flow at large Reynolds numbers', *J. Fluid Mech.*, **41**, 453–480 (1970).
11. P. Moin and J. Kim, 'Large eddy simulation of turbulent channel flow', *J. Fluid Mech.*, **118**, 341 (1982).
12. K. Horiuti, 'Large eddy simulation of turbulent channel flow by one-equation modeling', *J. Phys. Soc. Jpn.*, **54**, 2855–2865 (1985).

13. V. Schumann, 'Subgrid scale model for finite difference simulations of turbulent flows in plane channel and annuli', *J. Comput. Phys.*, **18**, 376–404 (1975).
14. A. Baker, *Finite Element Computational Fluid Mechanics*, McGraw-Hill, New York, 1985.
15. C. G. Speziale, 'Turbulence modeling in non-inertial frames of reference', *ICASE Report 88.18*, 1988.
16. B. E. Launder and D. B. Spalding, *Mathematical Models of Turbulence*, Academic Press, New York, 1972.
17. W. Rodi, 'Turbulence models and their application in hydraulics', *International Association for Hydraulic Research, State-of-the-art Paper*, Delft, 1980.
18. A. G. Hutton, R. M. Smith and S. Hickmott, 'The computation of turbulent flows of industrial complexity by the finite element method. Progress and prospects', *Finite Elements in Fluids, Vol. 7*, Chap. 15, Wiley, 1987.
19. C. Bègue, B. Cardot and O. Pironneau, 'Simulation d'écoulements turbulents à moyenne instationnaire', *INRIA Report 914*, 1988.
20. D. Maclaughin, G. Papanicolaou and O. Pironneau, 'Convection of micro-structures', *SIAM J. Appl. Math.*, **45**, 780–796.
21. T. Chacon, 'Oscillations due to the transport of micro-structures', *SIAM J. Appl. Math.*, **48**, 1128–1146 (1989).
22. N. Ukeguchi, H. Sataka and T. Adachi, 'On the numerical analysis of compressible flow problems by the modified "flic" method', *Comput. Fluids*, **8**, 251 (1980).
23. J. Douglas and T. F. Russell, 'Numerical methods for convection dominated diffusion problems based on combining the method of characteristics with finite element methods or finite difference method', *SIAM J. Numer. Anal.*, **19**, 871–885 (1982).
24. J. P. Benqué, O. Daubert, J. Goussebaile and H. Haugel, 'Splitting up techniques for computations of industrial flows', in A. V. Balakrishnan (ed.), *Vistas in Applied Mathematics*, Optimization Software Inc., Springer, New York, 1986.
25. O. Pironneau, 'On the transport-diffusion algorithm and its applications to the Navier–Stokes equations', *Numer. Math.*, **38**, 309–332 (1982).
26. R. Glowinski, *Numerical Methods for Nonlinear Variational Methods, Springer Series in Computational Physics, Vol. 13*, Springer, Berlin, 1984.
27. J. Cahouet and J. P. Chabart, 'Some fast 3-D finite element solvers for generalized Stokes problem', *Rapport EDF HE/41/87.03*, 1987.
28. J. Goussebaïle and A. Jacomy, 'Application à la thermo-hydrolique des méthodes d'éclatement d'opérateur dans le cadre éléments finis: traitement du modèle k–ε', *Rapport EDF-LNH HE/41/85.11*, 1985.
29. C. Parès 'Un traitement faible par élément finis de la condition de glissement sur une paroi pour les équations de Navier–Stokes', *Notes C. R. Acad. Sci., I.*, **307**, 101–106 (1988).
30. O. Pironneau, 'Conditions aux limites sur la pression pour les équations de Navier–Stokes, *Notes C. R. Acad. Sci. I*, **303**, 403–406 (1986).
31. C. Bègue, C. Conca, F. Murat and O. Pironneau, 'A nouveau sur les équations de Navier–Stokes avec conditions aux limites sur la pression', *Notes C. R. Acad. Sci., I*, **304**, 23–28 (1987).
32. C. Bègue, C. Conca, F. Murat and O. Pironneau, 'Equations de Navier–Stokes avec conditions aux limites sur la pression', in H. Brezis and J. L. Lions (eds), *Nonlinear Partial Differential Equations and their Applications, Collège de France Seminar* **9**, Pitman, 1988.
33. G. Comte-Bellot, 'Ecoulement turbulent entre deux parois planes', *Publications Scientifiques et Techniques du Ministère de l'Air*, Internal Publications, Paris, 1980.
34. P. L. Viollet, 'On the modeling of turbulent heat and mass transfers for computations of buoyancy affected flows', *Proc. Int. Conf. on Numerical Methods for Laminar and Turbulent Flows*, Venice, 1981.
35. B. Cardot, *Thesis*, University of Paris 6, 1989.
36. O. Ortegon, 'Tabulation of the closure tensors for the MPP turbulence model', *INRIA Report 757*, 1987.